ELSEVIER

A-type granites and related rocks: petrogenesis and classification

A.V. Grebennikov [a,b,*]

[a] Far Eastern Geological Institute, Far Eastern Branch of the Russian Academy of Sciences, pr. 100-letiya Vladivostoka 159, Vladivostok, 690022, Russia
[b] Far Eastern Federal University, ul. Sukhanova 8, Vladivostok, 690950, Russia

Abstract

The problems of identification of A-type granitoids are analyzed. These rocks occur in different geodynamic settings. Owing to their mantle nature, they show distinct REE specialization. These are acid intrusive rocks, whose volcanic products are of crucial scientific and practical significance. However, neither the great number of proposed classification schemes and diagrams, including those based on expensive analytical data, nor hot scientific discussions of their identification and the ambiguity of the term A-granitoids helped to determine their classification features in full measure. A principally new discriminant diagram is proposed for the classification of igneous A-type rocks, based on the analysis of earlier obtained results and the petrochemical composition of these rocks. A comparative analysis of subdivision of granites and related felsic volcanic rocks ($SiO_2 > 67$ wt.%), based on the ternary $(Na_2O + K_2O)–Fe_2O_3^* \times 5–(CaO + MgO) \times 5$ and other widely applied diagrams, has shown the advantage of the proposed discriminant diagram for the classification of A-type granitoids from different geodynamic settings.

Keywords: A-, S-, and I-type granites and rhyolites; petrochemical classification; tectonic settings

Introduction

Igneous rocks, often present in anorogenic environments and having an anhydrous alkaline aluminous composition, have been hotly discussed for years and are considered ambiguous. Before proceeding to the analytical review of research data on these rocks, let us dwell on the term A-type granites. In the world literature (and in this paper) it is used as a collective term for a particular type of felsic igneous rocks, because it equally corresponds to intrusive and igneous products of felsic magmatic melts widespread both in space and in time. In numerous literature works on petrology, geochronology, geochemistry, and metallogeny of A-type granites as well as International Project IGCP 510 (Global Correlation of A-type Granites and Related Rocks, their Mineralization, and Significance in Lithospheric Evolution), geologists came to the conclusion that most of the problems on the recognition of distinctive features of these rocks are still unsolved. Moreover, the existing classification schemes for A-type granitoids are so complicated and contradictory that their application is rather difficult. In this paper we review the state of the problem, based on analysis of scientific literature on felsic igneous A-type rocks, and propose our maximally simplified petrochemical discriminant diagram for their separation. We also consider the possibility of using it as a tool for a comprehensive analysis of igneous complexes for petrogenetic and geodynamic constructions.

The state of the art of the problem

Introduction of the term A-type granites is attributed to M. Loiselle and D. Wones, who proposed it at the conference of the US Geological Survey in 1979. They applied this term to anorogenic granites of moderate alkalinity, crystallized at low water and oxygen fugacity from melts and high HF/H_2O ratio (Loiselle and Wones, 1979). Such rocks were found in rift zones and stable blocks of the Earth's crust. It is worth noting that at the same conference, Chappell and White (1974), the founders of the alphabetical classification of granitoids, made a generalized report, where they presented a genetic scheme comprising four main types of granites differing in the composition and source of rocks. In addition to the already known S(peraluminous)- and I(calc-alkaline)-types, they included M-type granites (products of mantle melts) and non-classified anorogenic granites that corresponded to present-day A-type granites. Though White proposed the term R-type granites for them, based on their generation from residual melt (Bonin, 2007), it was too general and was not recognized in

* Corresponding author.
E-mail address: greandr@hotmail.com (A.V. Grebennikov)

the scientific world. The first paper where the term *A*-type granites was used was written by Collins et al. (1982). The authors assigned the granite complexes of Southeastern Australia to the *A*-type, based on the high contents of Nb, Ga, Y, and REE and low contents of Al(!), Mg, and Ca. The early crystallization of amphibole (hastingsite) and the late crystallization of biotite (annite) were explained by the authors by the enrichment of magmatic melts with F and Cl. They were the first to establish that high Ga/Al ratios are a specific feature of *A*-type melts, which was later illustrated by classification diagrams (Whalen et al., 1987). Based on the Ga/Al ratio and contents of Zr, Nb, Ce, and Y, empirical fields for *A*-type granites and most of orogenic granitoids were constructed. Unfortunately, the fields of highly differentiated *I*- and *S*-type quartz-feldspathic granitoids partly overlap the field of *A*-type granites on these diagrams.

For a long time (as well as today), the geologists identified *A*-type granitoids as within-plate granitoids (WPG), based on their geochemical composition. On the diagrams constructed by Pearce et al. (1984) and Harris et al. (1986), these rocks fell mainly in the field of WPG. Taking into account the high total contents of $Na_2O + K_2O$, or, more correctly, the peralkaline composition of these melts $(Na + K > Al)$, Maeda (1990) proposed a new classification diagram to separate *I*-, *S*-, and *A*-type granites. Note that the above classifications, complementing each other in many respects, distinctly separate felsic igneous rocks of mantle genesis, e.g., alkaline rhyolites (comendites and pantellerites), from crustal melts (*I*- and *S*-type rocks). At the same time, they do not take into account the diversity of these unique products of magmatic melts. Comendites (less alkaline and ferroan but more aluminous rhyolites) were found on volcanic islands located across mid-ocean ridges (Ascension, Bouvet, Easter, Pitcairn, etc.) and on continents, where they are confined to large rift systems (Kenya, Ethiopia) or the sites of large tectonic dislocations (western USA, Australia). Pantellerites (more alkaline and ferroan but less aluminous rhyolites) are usually observed on continental rifts (East African, Red Sea) and on oceanic islands being an extension of sea plateaus (Grand Canary, Kerguelen, the Azores). Comendites and pantellerites seldom occur together. They were found within the same volcano only in the Afar Ridge region, Ethiopia.

As for peraluminous *A*-type granites, represented by rapakivi and similar rocks of crustal genesis, their composition points usually lie near the WPG–VAG (volcanic-arc granites) boundary domain (Pearce et al., 1984) or near the FG (fractionated granites) domain (Whalen et al., 1987). Thus, these granites were not quite consistent with the definition of the *A*-type accepted at that time. Therefore, it was proposed to use the term "postcollisional" as an analog of *A*-type granites because of their abundance in different collision environments (Sylvester, 1989). At the same time, Maniar and Piccolli (1989) proposed a new series of discriminant diagrams for the separation of granitoids. Among anorogenic complexes, they recognized rift granitoids, granitoids of continental epeirogenic uplifts, and oceanic plagiogranites. However, there was no place for postcollisional granitoids in their classifica-

tion as well as on the diagrams of Pearce et al. (1984). Rogers and Greenberg (1990) attempted to unite these granite varieties by recognizing postorogenic and anorogenic *A*-granitoids: granites of anorthosite complexes (rapakivi) and alkali granites of ring complexes, i.e., based exclusively on their geodynamic settings rather than their geochemical parameters.

Special attention should be given to the research by Eby (1992), Professor from the University of Massachusetts, who divided *A*-type granitoids into two groups according to the contents of trace elements (Y, Nb, Ce, and Ga), in particular, Y/Nb. Note that the diagram proposed by Eby could have been used only for rocks falling in the fields of WPG on the diagrams of Pearce et al. (1984) and in the fields of *A*-type granites on the diagrams of Whalen et al. (1987). The group of granites with low Y/Nb (<1.2) includes felsic igneous rocks of oceanic islands and continental rifts of anorogenic settings. It was assumed that this type of rocks formed from oceanic-island basalts (OIB) in within-plate or rift settings. Granites with higher Y/Nb, corresponding to a wide range of geodynamic settings (including collision and exceptive anorogenic rapakivi granite ones), were produced from basalts of continental margins and island arcs (IAB) or as a result of the partial melting of the crust. Eby drew the crucial conclusion that *A*-type granitoids might be produced in different ways, not always corresponding to the anorogenic regime. For example, he established that not all granites of group A_1 are the products of *M*-type melts and granites of group A_2 are the subtype of *I*-type granites, as was earlier believed by Collins et al. (1982). Indeed, repeated generation of magmatic melts from the crust that has already underwent partial melting and thus is poor in Si, K, and Fe/Mg should result in different contents of these elements in *A*-type granites. Unfortunately, Eby's data, which surely played a crucial role at the first stages of the research, do not permit *A*-type granites to be separated into two discrete groups. More likely, they demonstrate the conjugate fields of postcollisional and postorogenic (up to within-plate) granitoids and form a field of uncertainty along the A_1–A_2 boundary (Bonin (2007). Hence, this diagram must be used with great caution, especially when drawing conclusions about the sources of magmatic melts.

Barbarin (1999) chose another approach. He used a complex of criteria (mineralogical, geological, and geochemical, including isotope ones) to separate granite series and thus to establish the genesis of magmas and the geodynamic settings of their formation. He recognized orogenic calc-alkaline peraluminous (*S*-type) and mid-ocean tholeiitic granitoids. Unfortunately, he included only peralkaline *A*-type granites of mantle genesis into his classification but ignored *A*-granitoids of crustal origin.

Based on the experience and more than twenty genetic schemes of previous researchers, Frost et al. (2001) proposed a specific classification of felsic igneous rocks according to their petrochemical composition. He took three chemical parameters as a basis: (1) index $FeO^*/(FeO^* + MgO) > 0.486 + 0.0046 \times SiO_2$ wt.%, permitting separation of magnesian and ferroan (*A*-type) granitoids, (2) Peacock modified alkali–lime index $(Na_2O + K_2O–CaO)$ (MALI), and (3) alumina saturation
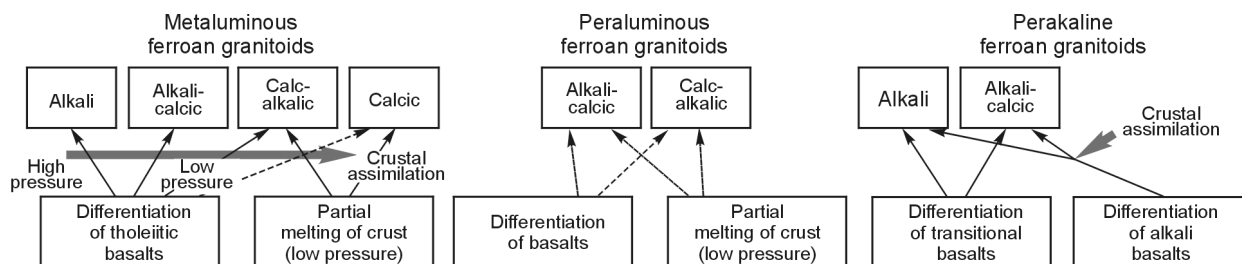
Fig. 1. Scheme illustrating petrogenesis of ferroan granitoids of different types (Frost and Frost, 2011).

index (ASI) Al/(Ca–1.67×P + Na + K), permitting division of felsic igneous rocks into peraluminous (ASI > 1.0), metaluminous (ASI < 1.0, (Na + K) < Al), and peralkaline (ASI < 1.0, (Na + K) > Al) ones. Using these diagrams, the authors recognized the fields of *A*-type granitoids and also divided the latter into eight geochemical groups of different origin and evolution (Frost and Frost, 2011). For example, they showed that ferroan metaluminous granitoids might have formed as a result of the differentiation of tholeiitic basalts. During the partial melting, the granitic crust became enriched with alumina. Low-pressure melting of quartz–feldspathic rocks might have led to the crystallization of calc-alkaline metaluminous granitoids. Differentiation of basaltic magmas of alkaline or intermediate compositions, accompanied by the crustal assimilation, resulted in peralkaline granitoids (Fig. 1).

Considering the known classification schemes, we should mention the discriminant diagram proposed by Velikoslavinskii (2003), which takes into account a great number of empirical data on the geochemical composition of felsic igneous rocks and thus is more appropriate for the geodynamic typification. Though the binary plot presented by the author has no direct relation with *A*-type granitoids, it clearly separates the fields of within-plate, collision, and subduction granitoids. Unfortunately, the wide spectrum of geochemical data, the main requirement for construction of the plot, is difficult to realize in practice:

$X = (196.203 \times SiO_2) + (753.953 \times TiO_2) + (481.96 \times Al_2O_3) + (92.664 \times FeO) + (521.5 \times MgO) + (374.766 \times CaO) + (7.571 \times Na_2O) - (584.778 \times K_2O) - (0.379 \times Ba) - (0.339 \times Sr) - (0.733 \times Rb) - (0.429 \times La) - (3.33 \times Ce) - (5.242 \times Nd) + (10.565 \times Sm) - 19,823.8;$

$Y = (1292.962 \times SiO_2) + (4002.667 \times TiO_2) + (1002.231 \times Al_2O_3) + (1297.136 \times FeO) + (262.067 \times MgO) + (1250.48 \times CaO) + (1923.417 \times Na_2O) + (1009.287 \times K_2O) + (0.3634 \times Ba) - (0.325 \times Sr) - (0.701 \times Rb) + (0.8015 \times La) + (3.347 \times Ce) + (2.68 \times Nd) + (10.11 \times Sm) - 126,860.$

In recent time, there is a tendency in non-Russian literature for constructing universal diagrams for separation of igneous rocks (including granites) depending on their geodynamic settings. Unfortunately, such plots require not only a particular statistic processing but also a difficult labor-consuming conversion of analytical data. One of such diagrams has recently been published by Verma et al. (2013):

$X = (0.051 \times \ln(TiO_2/SiO_2)_{adj}) + (0.226 \times \ln(Al_2O_3/SiO_2)_{adj}) + (-1.77 \times \ln(Fe_2O_3/SiO_2)_{adj}) + (1.83 \times \ln(FeO/SiO_2)_{adj}) + (-0.065 \times \ln(MnO/SiO_2)_{adj}) + (0.134 \times \ln(MgO/SiO_2)_{adj}) + (0.225 \times \ln(CaO/SiO_2)_{adj}) + (0.742 \times \ln(Na_2O/SiO_2)_{adj}) + (-1.78 \times \ln(K_2O/SiO_2)_{adj}) + (0.146 \times \ln(P_2O_5/SiO_2)_{adj}) - 2.12;$

$Y = (1.09 \times \ln(TiO_2/SiO_2)_{adj}) + (-1.65 \times \ln(Al_2O_3/SiO_2)_{adj}) + (-1.19 \times \ln(Fe_2O_3/SiO_2)_{adj}) + (1.03 \times \ln(FeO/SiO_2)_{adj}) + (0.82 \times \ln(MnO/SiO_2)_{adj}) + (0.026 \times \ln(MgO/SiO_2)_{adj}) + (0.223 \times \ln(CaO/SiO_2)_{adj}) + (0.212 \times \ln(Na_2O/SiO_2)_{adj}) + (0.085 \times \ln(K_2O/SiO_2)_{adj}) + (-0.85 \times \ln(P_2O_5/SiO_2)_{adj}) + 2.54.$

One else aspect of study and classification of *A*-type granitoids is their common interpretation as reduced products of melts. Consequently, the existence of magnetite series among *A*-type granites was paid little attention because these series did not meet the precise definition of *A*-type granites but corresponded more to calc-alkaline (orogenic) *I*-granites. These granites, containing modal magnetite, were first described as an *A*-type in the USA (Anderson and Bender, 1989). In 2007, Brazilian scientists, studying granitoids of magnetite series from the Amazon River basin, also established high *f* values of the bulk rock and of the hosted biotite and amphibole, which suggests crystallization of the corresponding melts in relatively reducing conditions (Dall'Agnol and Olivera, 2007). This made them conclude that the magnetite and ilmenite series (according to the definition by Ishihara (1977)) are not always equivalent to oxidized and reduced *A*-type granitoids. For these rocks, the authors introduced the term "oxidized *A*-type" and assumed their crystallization from hydrous magmas (≥4 wt.% H_2O), which were probably generated from quartz–feldspathic rocks of the lower crust. The refining term "oxidized *A*-type" introduces still more uncertainty in the definition of *A*-type granitoids, because most of the above-discussed classifications cannot distinguish between such rocks and both *A*-type granites and orogenic calc-alkaline *I*-type granites.

To sum it up, let us mark major features of *A*-type granitoids. Their associations were mapped on all continents (including Antarctica), and the time of their formation varies from Neoarchean (~2.7 Ga) to Cenozoic (10 Ma and younger). They are rather rare in the lower crust (like, e.g., some charnockite complexes) but are typical of subsurface subvolcanic levels, forming circular root feeders of calderas. These granitoids are usually classified as quartz syenites and metaluminous and peralkaline granites, and their volcanic analogs are treated as vitrophyric rhyolites, comendites, and pantel-

lerites. They have an alkaline calcic to alkaline ferroan bulk composition, high contents of LILE, HFSE (first of all, Nb, Ga, and Y), and REE (except for Eu), and low contents of Sr, Sc, and V and are rich in halogens, especially F. *A*-type granites are easily recognizable by mineral composition: the presence of ferroan silicates (ferrohedenbergite, ferrohastingsite, fayalite, and annite) or aegirine, arfvedsonite, and riebeckite (in agpaitic granites) as well as feldspar. Since *A*-type granites are observed in association with mafic igneous rocks both on the continents and on the ocean bottom, they are regarded as mantle products of alkaline melts. Their Rb/Sr and Sm/Nd isotope ratios testify to the presence of mantle melt traces. They are characterized by a high metal potential, which was first noted during the investigation into Nigerian granites (Bowden et al., 1987). Besides F, Y, Zr, and REE, *A*-type granites are known as sources of Sn, W, Ta, Nb, and Be. Sn–In mineralization is specific for only the topaz garnets of Northeastern and Central Brazil (Botelho and Moura, 1998). FeO–Cu–Au mineralization is paragenetically related to the *A*-type granites of Missouri, USA (Kisvarsanyi and Kisvarsanyi, 1990) and Australia (Pollard, 2006). These granites form in different geodynamic conditions, from within-plate ones to plate sliding boundaries. *A*-type granites and rhyolites are often associated with mantle plume, e.g., the Yellowstone fayalite rhyolites. They occur in areas of continental rifting (e.g., granite complexes of Africa, South America, and northeastern USA, related to the opening of the Atlantic Ocean) and are also associated with complexes in zones of large-scale continental extensions (Basin and Range province on the western periphery of the USA).

Methods and results of study

A universal diagram for distinguishing *A*-type granitoids from other types was constructed using an approach competing with the popular opinion that the specific features of igneous rocks cannot be recognized because of the negligible difference in the composition of the major oxides in rocks with similar SiO_2 contents. However, the existing classifications of granitic rocks, based on the contents of dispersed and trace elements, do not ensure their unambiguous identification as regards their source and tectonic setting (Frost et al., 2001) because dispersed elements in felsic melts (in contrast to basalts) are usually incompatible (Bea, 1996). Rare-earth elements, U, Th, and Zr are present mainly in accessory minerals: apatite, zircon, sphene, orthite, and monazite. Other elements, including Nb and Y, concentrate in oxides and amphiboles; their contents reflect the history of crystallization and some intensive parameters (oxygen and water fugacity). Crustal contamination also exerts a stronger effect on the contents of dispersed elements in granitic melts as compared with more mafic melts. Thus, the choice of rock-forming elements as a basis for classification of granites is reasonable.

The main petrochemical parameter of *A*-type granites is their *f* value. Frost and Frost (2011), following Creaser et al. (1991), noted that the term *A*-type lost its original meaning

for 30 years and today it is more appropriate to call such igneous rocks ferroan. This term exactly defines the composition and major distinctive features of rocks. In our opinion, the ferroan composition of melts producing *A*-type granites is due to extremely low (often close to zero) contents of Mg rather than high contents of FeO and Fe_2O_3. The extremely low contents of Ca (thermophile element) and high contents of Na and K are an additional specific feature of *A*-type granites. The regular proportions of these elements in *A*-type melts served as a basis for constructing discriminant diagrams in this study.

The diagrams are based on published data on the chemical composition of *A*-type rocks (a total of >900 analyses, including 185 for oxidized *A*-type granites), which depict the characteristics of their different facies types (granites, tuffs, ignimbrites, lavas, extrusive bodies) from the world-famous occurrences (including the parameters taken into account in the rock classifications (Eby, 1992; Frost et al., 2001; Whalen et al., 1987)). For comparison, the results of ~600 chemical analyses of granitoids of other types (including *S*- and *I*-types) were added to the database (Table 1). We included only igneous rocks with $SiO_2 > 67$ wt.% that were not subjected to secondary alterations, with LOI ≤ 4 wt.%. The analytical consuderable results for glass fragments, fiamme, and extreme varieties (end-members of highly differentiated melts and liquation products) were excluded from the data sample. The compositions were converted for anhydrous residue and reduced to 100%. The molecular quantities were calculated by standard techniques (Chetverikov, 1956).

The ternary diagram $(Na_2O + K_2O)$–$Fe_2O_3^* \times 5$–$(CaO + MgO) \times 5$, based on the molecular quantities of rock-forming elements (Fig. 2*a*), is the most informative among the numerous constructed empirical schemes. It ensures a more effective separation of varieties of *A*-type granitoids recognized by Eby (1992) (Fig. 2*b*).

The compositions of different facies types of igneous rocks (~1500 chemical analyses) form three main fields on the above diagram (Fig. 3*a*). Two fields (A_1, A_2) correspond to felsic magmatic *A*-type rocks of different ages and geodynamic settings (Table 1). They are noticeably separated (with a negligible (~2–3%) overlapping) from the rest types of felsic igneous rocks, including *I*- and *S*-type granites of island arcs and active continental margins. An interesting crucial feature of the diagram is the clustering of composition points of *A*-type granites from each occurrence in only one field (Fig. 3*b*). The only exclusion is the West Yemen subsolvus and hypersolvus granites (Table 1). However, the duality of their composition and of the genesis and depth of generation of magmatic melts was noted by many researchers (Capaldi et al., 1987; Tommasini et al., 1994). Moreover, the initial Sr isotope ratios in the rocks of the fields A_1 and A_2 show a common regularity. For example, the rocks of the field A_1 are characterized by lower $(^{87}Sr/^{86}Sr)_I$ ratios, whereas the compositions of rocks of the field A_2 testify to the significant effect of assimilation by crustal material on the rock formation (Table 1, Fig. 3*c*). It is remarkable that the Sr isotope ratios in the lower parts of A_2-type volcanic sections are usually

Table 1. Different types of felsic igneous rocks and their characteristics

Locality	Characteristics	Age, isotope composition	Reference
A1-type granites			
Oceanic islands	Comendites of Easter, Ascension, Bouvet, Hrafntinmusker, and Gran Canaria Islands; pantellerites of Socorro, Lisiscard, Barranco del Taurito, and Santa Barbara Islands; comendites and pantellerites of Papua New Guinea, Mayor, and other islands of northern New Zealand	from 3000 to 300 ka, $^{87}Sr/^{86}Sr_I = 0.7050$	(Baker, 1974; Karsten et al., 1974; Smith et al., 1977)
Pantelleria Island (Mediterranean Sea)	Perakaline trachytes and pantellerites	~ 50–45 ka	(Avanzinelli et al., 2004)
Corsica Island (Mediterranean Sea)	Albite–riebeckite–aegirine granites	~ 246 Ma, $^{87}Sr/^{86}Sr_I = 0.7034$	(Bonin et al., 1978)
Kerguelen Plateau (southern Indian Ocean)	Trachytic and rhyolitic lavas and clastic rocks	~ 68 Ma, $^{87}Sr/^{86}Sr_I = 0.7054–0.7059$	(Barron et al., 1991; Kieffer et al., 2002)
Northeastern USA, New Hampshire (The White Mountain Batholith)	Quartz syenites and riebeckite granites	~ 200–155 Ma, $^{87}Sr/^{86}Sr_I = 0.7031$	(Eby et al., 1992)
Malawi, East African Rift (Chilwa Alkaline Province)	Amphibole–pyroxene and aegirine–riebeckite granites	~ 135–105 Ma	(Woolley and Jones, 1987)
Ethiopia, East African Rift (Asela–Ziway area)	Ignimbrites of pantellerites and, seldom, comendites	~ 1.8–0.2 Ma, $^{143}Nd/^{144}Nd_I \approx 0.51278$	(Trua et al., 1999)
Kenya, East African Rift (Naivasha Rhyolite Complex)	Comendites: extrusions, and lava flows	~ 15 ka, $^{87}Sr/^{86}Sr_I = 0.7055–0.7073$	(MacDonald et al., 1987)
Northeastern and northern Nigeria (Nigerian Younger Complex)	Albite–riebeckite and arfvedsonite granites	160–150 Ma	(Orajaka, 1986; Ogunleyea et al., 2005), http://research.gg.uwyo.edu/granite/granites/
Sudan (Ras ed Dom Ring Complex)	Syenites and alkali granites	~ 236 Ma, $^{87}Sr/^{86}Sr_I = 0.7056$	(O'Halloran, 1985)
Western Yemen, Arabian Peninsula (Trap Series of the Afro–Arabian Plate)	Arfvedsonite granites	~ 23–20 Ma, $^{87}Sr/^{86}Sr_I = 0.7040–0.7050$	(Capaldi et al., 1987)
Saudi Arabia, Arabian Peninsula (Hadb Aldyaheen, Jabal Sayid Complexes)	Riebeckite granites	573–557 Ma	(Radain et al., 1981)
Volcano Pektusan (Northern Korea–China boundary)	Ignimbrites and tuffs of trachyrhyolite, comendite, and pantellerite compositions	3 Ma–1702 yr, $^{87}Sr/^{86}Sr_I = 0.7054$	(Popov et al., 2005)
Mongolo–Transbaikalian belt of granitoids (Bryansky complex)	Aegirine–riebeckite granites, comendites, and trachyrhyolites	279–285 Ma, $^{87}Sr/^{86}Sr_I = 0.7050–0.7053$	(Dobretsov, 2003; Litvinovsky et al., 2002)
A2-type granites			
South Greenland (Gardar Province)	Alkali granites	~ 1150 Ma, $^{87}Sr/^{86}Sr_I = 0.7083$	(Goodenough et al., 2000)
Western USA, Idaho, Utah, and Nevada	Topaz rhyolites of extrusive domes	from 50 to 0.6 Ma, $^{87}Sr/^{86}Sr_I = 0.7100$	(Christiansen et al., 2007)

Table 1 (*continued*)

Locality	Characteristics	Age, isotope composition	Reference
A2-type granites			
Western USA, California (Death Valley Region)	Biotite–hornblende rapakivi granite	12.4–9.8 Ma, $^{87}Sr/^{86}Sr_I = 0.7059–0.7126$	(Calzia and Ramo, 2005)
Western USA, California (Coso Volcanic Field)	Rhyolites of extrusive domes and lava flows	from 1040 to 60 ka, $^{87}Sr/^{86}Sr_I = 0.7055$	(Bacon et al., 1981)
USA, Wyoming (Yellowstone)	Lavas, ignimbrites, and volcanic glasses of rhyolites	from 10 to 0.07 Ma, $^{87}Sr/^{86}Sr_I = 0.7081–0.7185$	(Cathey and Nash, 2004; Girard and Stix, 2010; Pritchard and Larson, 2012)
USA, Wyoming (Sherman Batholith)	Biotite–hornblende rapakivi granite with fayalite	~ 1430 Ma, $^{87}Sr/^{86}Sr_I = 0.7065–0.7309$	(Frost et al., 1999)
Central USA, Colorado (Pikes Peak)	Biotite–amphibole, fayalite, and riebeckite granites	~ 1080 Ma, $^{87}Sr/^{86}Sr_I = 0.7100$	(Smith et al., 1999)
Southeastern Australia (Gabo, Mumbulla Suites, Narraburra Granite)	Riebeckite and biotite granites; aegirine and arfvedsonite granites	Early and Late Devonian	(Collins et al., 1982; Wormald and Price, 1988)
Northwestern India, Rajasthan; southeastern India (Chimakurti, Errakonda, Uppalapadu Plutons)	Albite–amphibole granites;ferrosyenites	~ 1780 Ma; ~ 1352 Ma, $^{87}Sr/^{86}Sr_I = 0.7217–0.7734$	(Kaur et al., 2006; Kumar et al., 2007)
Northeastern China (Qianshan pluton)	Biotite and amphibole granites	~ 126 Ma, $^{87}Sr/^{86}Sr_I = 0.7215–0.7283$	(Yang et al., 2006)
Western Yemen, Arabian Peninsula	Granites with biotite and calcic amphibole	~ 23–20 Ma, $^{87}Sr/^{86}Sr_I = 0.7059–0.7212$	(Capaldi et al., 1987; Tommasini et al., 1994)
Egypt, southern Sinai (Katherina Volcanics)	Alkaline rhyolites, lavas, and pyroclastics	590–560 Ma, $^{87}Sr/^{86}Sr_I \approx 0.7062$	(Azer, 2007)
Russian Far East, Primorye (Eastern Sikhote-Alin)	Tuffs, ignimbrites, rhyodacite and rhyolite lavas (Bogopol volcanic complex)	~ 59–50 Ma, $^{87}Sr/^{86}Sr_I = 0.7068–0.7081$	(Grebennikov, 2003; Grebennikov and Maksimov, 2006; Grebennikov and Popov, 2014; Mikhailov, 1989)
Russian Far East, Kamchatka Peninsula (Sredinnyi Ridge)	Comendites, dikes, and subvolcanic bodies (Volcanoes Belogolovskii, Nyulkandya, and Cherpuk)	Pliocene–Quaternary, $^{87}Sr/^{86}Sr_I \approx 0.7062$	(Patoka, 1983; Pokrovskii, 2000)
Borthwestern Namibia (Gross Spitzkoppe and Klein Spitzkoppe Stocks)	Biotite and hornblende–biotite topaz–fluorite granites	~ 135–125 Ma, $^{87}Sr/^{86}Sr_I = 0.7100–0.7160$	(Frindt et al., 2004; Haapala et al., 2007)
Seychelles	Riebeckite and biotite granites	~ 570 Ma, $^{87}Sr/^{86}Sr_I = 0.7275$	(Suwa et al., 1994)
Eastern Bolivia (Velasco Alkaline Province)	Riebeckite and biotite granites	~ 143–134 Ma, $^{87}Sr/^{86}Sr_I = 0.7060–0.7090$	(Fletcher and Beddoe-Stephens, 1987)
Central Europe (Czechia–Germany boundary)	Biotite granites, tuffs, ignimbrites, and rhyolite lavas	~ 325–295 Ma	(Breiter, 2012)
Southern part of the North Baikal volcanoplutonic belt (postcollisional complexes)	Quartz–feldspathic extrusive and blanket rhyolites, biotite leucogranites (Primorye complex)	~ 1849–1875 Ma, $^{143}Nd/^{144}Nd_I = 0.51122–0.51153$	(Donskaya et al., 2008; Savel'eva and Bazarova, 2012)

Table 1 (*continued*)

Locality	Characteristics	Age, isotope composition	Reference
A2-type granites			
Southwestern margin of the Siberian craton	Biotite and biotite–amphibole granites and leucogranites	Early Proterozoic, $^{143}Nd/^{144}Nd_I = 0.51109–0.51136$	(Turkina et al., 2006)
Eastern margin of the Siberian craton	Rhyolite–granites (Tyn'yar complex)	$\sim 276–268$ Ma, $^{87}Sr/^{86}Sr_I = 0.7030$	(Ivanov et al., 2012)
Yenisei Ridge	Leucogranites (Kutukas and Glushikha complexes)	$\sim 700–690$ Ma$\sim 750–720$ Ma	(Nozhkin et al., 2008; Vernikovskaya et al., 2007)
Upper Yana–Kolyma folded area	Alkali-feldspathic (aegirine–arfvedsonite) and microcline–albite granites	Neoproterozoic–Late Cretaceous, $^{87}Sr/^{86}Sr_I = 0.7030–0.7441$	(Trunilina et al., 2008)
Other types of granitoids: syncollisional, granites of volcanic arcs and continental margins (*S*- and *I*-types), etc.			
Cordilleras (western USA and northwestern Mexico)	Granodiorites and high-K granites	~ 117 Ma	http://research.gg.uwyo.edu/granite/granites
Andes (Chile, Bolivia, Argentina)	Ignimbrites of rhyodacites and rhyolites	Miocene–Quaternary	(Coira and Kay, 1993; Pichler and Zeil, 1971; Yarmolyuk and Kovalenko, 1987)
Caledonides (Ireland and Great Britain)	Granodiorites and high-K granites	~ 420 Ma	http://research.gg.uwyo.edu/granite/granites/
Leucogranites (Nepal, northern Portugal, USA)	Muscovite high-Si granites	from 1700 Ma to Miocene	http://research.gg.uwyo.edu/granite/granites/
Australia (Lachlan Fold Belt)	Hornblende and two-mica granites	$\sim 420–360$ Ma	(Chappell and White, 1988, 1992)
Kamchatka (Volcanoes Uzon and Semyachik)	Ignimbrites of rhyodacites and rhyolites	Late Quaternary	(Leonov and Grib, 2004)
Primorye (East Sikhote-Alin volcanic belt)	Tuffs, ignimbrites, rhyodacite and rhyolite lavas (Primorye, Kamenka, Upper Sobolevka, and Siyanovka volcanic complexes)	Turonian–Maastrichtian	(Grebennikov and Popov, 2014; Mikhailov, 1989)
North Sayan zone of West Sayan	Plagiogranites (Maina complex)	~ 524 Ma	(Rudnev et al., 2005)
Southern margin of the Siberian craton	Trondhjemites (Chuya complex)	~ 2019 Ma	(Donskaya et al., 2013)
Oxidized *A*-type			
Brazil (periphery of the Amazon Shield)	Anorthosite–hypersthene rapakivi granites	from 1880 to 580 Ma, $^{87}Sr/^{86}Sr_I = 0.7065–0.7130$	(Dall'Agnol and Olivera, 2007; Fraga et al., 2009; Janasi et al., 2009)
Southwestern Norway (layered intrusion)	Anorthosite–hypersthene rapakivi granites	~ 1500 Ma, $^{87}Sr/^{86}Sr_I = 0.7075–0.7200$	(Duchesne and Wilmart, 1997)
Finland, Russia	Rapakivi granites	from 2500 to 1540 Ma	(Elliott et al., 2005; Heilimo et al., 2009; Lauri et al., 2006; Vetrin, 2006)
South Tien Shan (Kokshaal Ridge)	Biotite–amphibole granites, topaz leucogranites, and rapakivi granites	296–279 Ma, $\varepsilon_{Nd} = -1.6$ to -6.9	(Konopelko et al., 2007)
Southern margin of the Siberian craton	Biotite–amphibole granites (Kutim complex)	~ 2020 Ma, $\varepsilon_{Nd} = 1.9–2.5$	(Donskaya et al., 2013)

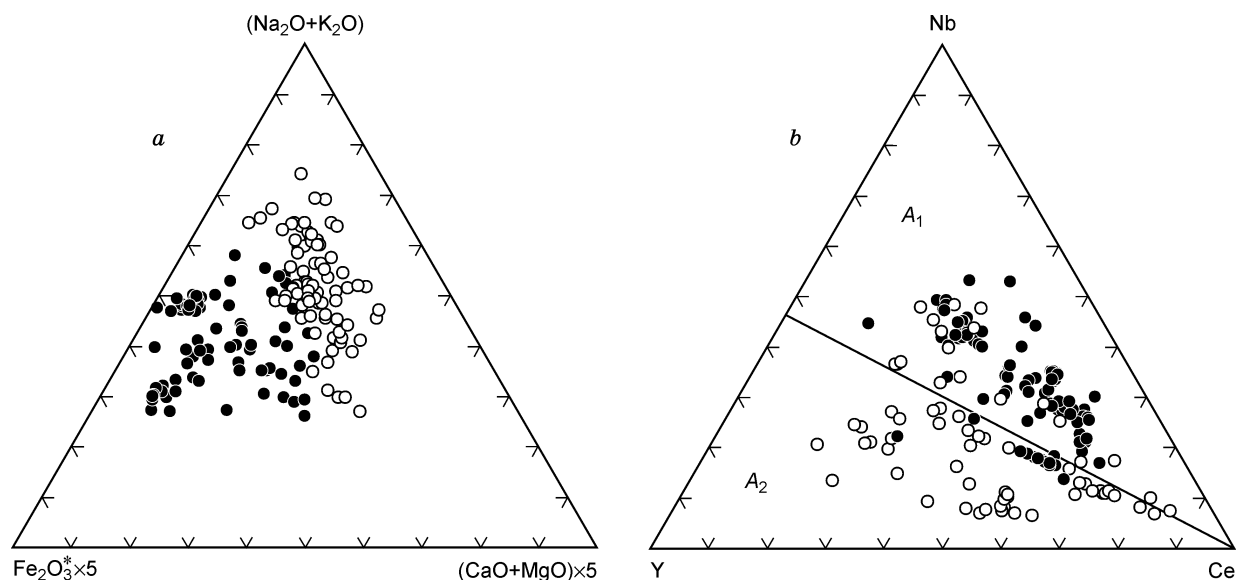Note. The names of the world-famous occurrences are given in English.

Fig. 2. Ternary petrogenetic diagrams: (*a*) (Na₂O + K₂O)–Fe₂O₃*×5–(CaO + MgO)×5 (mol. quant.); (*b*) Nb–Y–Ce (ppm) for *A*-type granites (Eby, 1992). A_1, Field of silicic rocks of oceanic islands, continental rifts, and hot spots (dark symbols), formed from within-plate or rift OIB; A_2, field of postcollisinal, postorogenic, and anorogenic granitoids (light symbols) formed from IAB and continental-margin basalts, from crustal tonalites and granodiorites, or through the partial melting of crust. Fe₂O₃*—as a total iron.

maximum and gradually decrease upsection (Grebennikov and Maksimov, 2006; Kuz'min, 1985). The diagram also shows the compositions of problematic oxidized *A*-type granitoids (Table 1) and magmatic melts of different geodynamic settings (data on melt inclusions (>2000 analyses) borrowed from Naumov et al. (2010)). All of them fall in the above two fields (Fig. 3*c*).

Discussion

Analysis of the data on the presented ternary diagram (Fig. 3) permits us to relate, with some caution, igneous complexes to a particular geodynamic setting because the geochemical features of granitic magmas reflect mostly the composition of their source. Moreover, volcanic facies (like intrusive ones) are complex products of intracrustal melts, basic magmas, and sedimentary substrate. No one diagram is so informative for understanding the genesis and geodynamic setting of formation of igneous rocks as a comprehensive analysis of data on their composition, isotope properties, structural position, and age. Therefore, only the general conclusions for each of the recognized groups of granites are presented below, and this diagram is proposed as one of the tools for a comprehensive analysis of igneous complexes.

Group A_1 is represented by granitoids of bimodal magmatic series formed in the setting of global continental and oceanic rifting. Group A_2 comprises felsic magmatic associations of local extension zones of intracontinental and continent-marginal areas. The former granitoids are, most likely, the result of the global horizontal crustal extension and expansion and the breaking of the continuity of lithospheric plates. The latter granitoids formed during rifting caused by the extension and thinning of continental crust (as a result of postsubductional

and postcollisional processes) with a partial breaking of its continuity (or without it) and the successive filling of the formed gaps with ascending hot mantle magma.

As follows from Table 1, A_1-type rocks form in within-plate magmatism settings: in the intracontinental system (oceanic islands) or near the divergent boundaries of lithospheric plates in cold intracontinental rifts, such as rift belts or triradiate-junction zones, where formation of igneous rocks is related to faulting and the relatively unobstructed penetration of mantle melts or plumes (Dobretsov, 2003). This is also evidenced by a great number of data of isotope studies (Table 1, references), which directly indicate the formation of felsic melts through the differentiation of alkaline or intermediate basaltic magmas and the minimum effect of their contamination with crustal material.

S- and *I*-type granites (resulting from the remelting of sedimentary or igneous rocks) depleted in mantle elements, on the contrary, melt out in the closed system near the convergent plate boundary, where the access of mantle matter is blocked by the subducting and/or stagnating slab of oceanic plate. These granites resulted from the intricate transformation processes in ascending primary magma. Seismotomographic data (Dobretsov et al., 2012) revealed five levels of melt formation: (1) dehydration and partial melting of slab with separation of melts (aqueous fluids) and their subsequent transition into the mantle wedge rocks; (2) formation of magma chambers and contamination of melts with mantle material; (3) formation of a large volatile-enriched chamber at the crust–mantle boundary; (4) formation of intracrustal chambers; and (5) formation of upper-crustal (0–5 km) chamber with subsequent assimilation and differentiation.

A_2-type granitoids, whose composition seems to be determined by the discrete permeability of lithospheric plates for mantle melts (considerably reduced fluids), bear traces of the
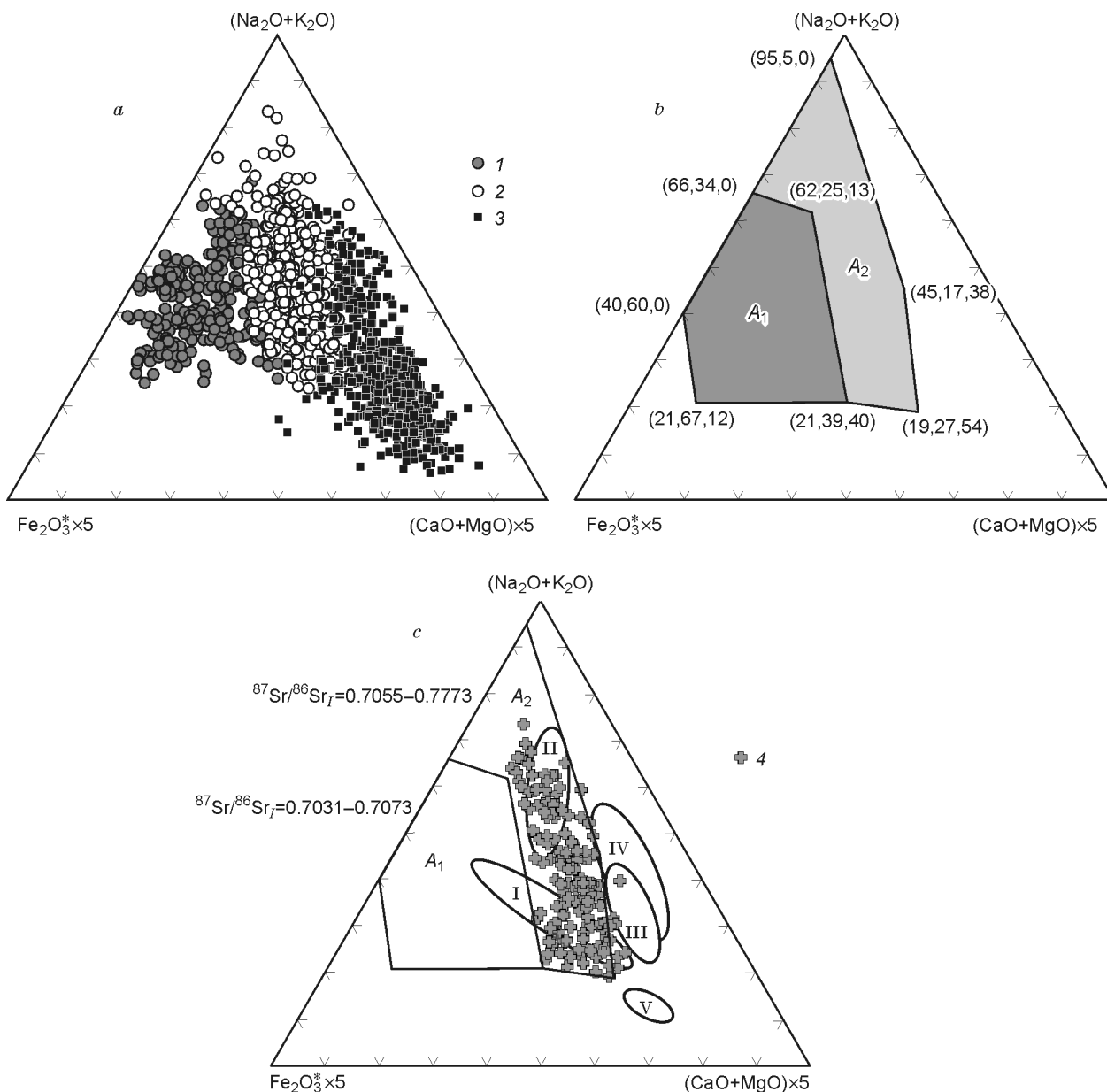
Fig. 3. Diagram (Na$_2$O + K$_2$O)–Fe$_2$O$_3^*$×5–(CaO + MgO)×5 (mol. quant.). *a–c*, For explanation, see the text. A_1, Field of silicic rocks of within-plate geodynamic settings: oceanic islands and continental rifts; A_2, felsic igneous rock associations of intracontinental and continental-margin geodynamic settings. The fields are separated by lines with coordinates (A_1: 40, 60, 0; 66, 34, 0; 62, 25, 13; 21, 39, 40; 21, 67, 12; A_2: 66, 34, 0; 95, 5, 0; 45, 17, 38; 19, 27, 54; 21, 39, 40; 62, 25, 13). Roman numerals mark the fields of felsic igneous rocks of major geodynamic settings, after Naumov et al. (2010): I, zones of mantle plumes in oceanic plates (oceanic islands and lava plateaus); II, intracontinental rifts and continental hot spots; III and IV, zones of subduction processes (III, zones of island-arc magmatism in oceanic crust; IV, zones of magmatism of active continental margins, involving continental crust in magma formation; V, back-arc spreading. *1, 2*, A_1- and A_2-type granites, respectively; *3*, other types of granitoids: syncollisional, granites of volcanic arcs and continental margins (*S*- and *I*-types), etc; *4*, oxidized *A*-type. Fe$_2$O$_3^*$—as a total iron.

interaction of crustal magmas with the enriched matter of the sublithospheric mantle and form in conditions different from those of A_1-type granites. For example, they form at the places (western USA, Far East of Russia, Southeastern Australia, etc.) where a global change in geodynamic setting takes place, when the orthogonal (counter) movement of plates at the convergent boundary (subduction) can give way to their shear relative to each other, i.e., the setting of a transform continental margin exists (Khanchuk et al., 1997). In this case, the subsided slab (part of the plate in the subduction zone) and oceanic plate (beyond the subduction zone) will have different

dynamic characteristics because of their location at different hypsometric levels. Therefore, at depths no greater than few tens of kilometers, the slab can break to form steeply inclined structures of shear extension, which ensure permeability for mantle material. Most likely, zones of transform faults subsided beneath the active continental margin (Egypt, western Yemen, eastern Bolivia, etc.) are the most favorable for the formation of mantle material feeders.

A_2-type granites can also form at the sites of convergent (collision) plate boundaries that are oriented at an angle (not orthogonally) to the direction of their movement. In this case,

there will be slips on the background of compression strains (transpression regime). This movement (in the postcollisional and late-collision settings) resulted in feathering extension structures striking in the direction of the plate motion. Such settings of *A*-type granite formation are specific for northwestern India, the Tien Shan, South Greenland, southwestern Siberian craton, etc.

In contrast to the above *A*-type granites revealed at the boundaries of lithospheric plates, there is one else group of A_2-granitoids localized in zones of intracontinental extension. One of such settings is the Yellowstone supercaldera, the largest volcanic system of North America, which formed above hot mantle jets (plumes) and is part (northeastern extension) of the Basin and Range Province (Smith et al., 2009), a classic example of intense shearing strains. Some authors (Best and Christiansen, 1991) think that such deformations are caused by the back rush or pinching of accreted oceanic slab at the postsubduction (postconvergent) stages, followed by its thinning and intense extension and by the upwarping of asthenospheric diapir that induced *A*-type magmatism. Others (Yarmolyuk and Kovalenko, 1991) relate these deformations to the subsidence of the spreading ridge beneath the continental plate. Overlapped mantle diapirs served as a source for crustal rifting and accompanying magmatism. The subsequent movement of the North American plate in the southwestern direction synchronously with intracontinental extension caused by a change in geodynamic regime (Jones et al., 1996) provoked the growth of mantle diapir (plume) curved northwestward. The diapir induced intense heating of continental lithosphere and the formation of the Yellowstone supercaldera filled with tuffs and lavas of *A*-type rhyolites.

Note that the extension regimes for the A_1- and A_2-type granitoids are significantly different. For example, Buck et al. (1988) considered two models of the formation of rift systems: "simple shear" and "pure shear". In the first case, there are shearing strains only in subhorizontal plane, and in the second, the crustal thinning is caused by extension in both directions. However, these deformation regimes depend mainly on the thermal state of crust rather than the stress conditions and the environment composition (Sklyarov et al., 1997). There are at least two types of deformations: brittle and plastic. In the case of brittle deformations and cold crust (classic continental rifting, A_1-type rocks), the interaction of mantle magmas with crustal material is minimum. If magmatic melt meets a hot viscous fluid (plastic) medium, it might stop and form intrusive bodies or an intermediate chamber and then break through them. This will cause a serious contamination of the melt (A_2-type rocks). Moreover, the shape of magmatic feeder also has a considerable effect on assimilation processes. In the case of vertical breakthrough of melt, the heat effect on the host rocks (few centimeters) is limited even for rock bodies tens of meters in thickness. If magma spreading takes place (resulting in lopolith, sill, etc.), the thickness of the heat effect zone increases by several orders of magnitude. As concluded by Sklyarov et al. (1997), there are magmas contaminated to different degrees depending on their localization in the heating zone. This largely complicates unambiguous determination of

the geodynamic setting based only on the geochemical compositions of igneous rocks. At the same time, the considered conditions largely determine the specific melting-out of *A*-type granitoids and their subdivision into A_1- and A_2-types.

As seen from the above diagram (Fig. 3), the main distinctive petrochemical feature of *A*-type granitoids is the ratio of bivalent to relatively small thermophile and large alkali cations. Transformation of rock (melt) with a similar inflow of some chemical components (SiO_2, Na_2O, and K_2O) and removal of others (MgO, FeO, CaO, etc.), known in literature as palyngenetic-metasomatic granite formation, is due to the specific fluid regime, namely, the impact of ascending transmagmatic solutions produced during the mantle outgassing. These fluids exhibit a well-expressed reducing potential, which is reflected in the mineral composition of *A*-type melts. The abundance of ferrohedenbergite, ferrohypersthene, highly ferroan biotite, and fayalite in volcanic analogs of *A*-type granites, the negligible contents of magnetite and high contents of ilmenite, the low degree of oxidation of volcanic glasses, and the presence of native iron, cohenite, and moissanite, together with chromatographic data, the composition of fluid and melt inclusions, and a considerable contribution of explosive processes to the volcanism suggest the presence of hydrogen (hydrocarbon or hydrofluorine) component in the fluid (Grebennikov et al., 2012). This hydrogen–hydrocarbon fluid causes depolymerization of siliceous melt (Bezmen et al., 2005), which favors amorphization of crystalline compounds. The latter process is caused by the reaction of hydrogen with silicate oxygen of these groups (Bogatikov and Borsuk, 1987), which weakens its bond with silicon and thus leads to the breaking of the groups, and even to their defluidization (vitrification, one else characteristic feature of *A*-type volcanics) as the temperature decreases. Depolymerization and destruction of, first of all, framework feldspathic sibotaxes under the action of water–hydrogen fluid as well as the leaching effect change the structural position of aluminum (its coordination number IV changes for VI). This plays the key role in the restructuring of melt and its viscosity decrease by several orders of magnitude (Epel'baum, 1980) and thus defines such an unusual set of mineral assemblages. The above specific mineral composition agrees with the theoretical and experimental conclusions drawn by Anfilogov et al. (1982).

Thus, the difference in the mineralogical and geochemical compositions of *A*-type granites and accompanying volcanics, from collisional granites of island arcs and continental margins (*S*- and *I*-types) to other felsic magmatic rocks near the convergent boundaries of lithospheric plates, is mainly due to differentiation of intracrustal melts with the active participation of reduced (essentially hydrogen) fluids supplied from the saturated sublithospheric-mantle material during the formation of felsic magmas. The difference in the compositions of A_1- and A_2-type granites (the latter are poorer in the mantle material) depends both on the permeability of the crustal material for mantle melts arriving at the upper hypsometric lithospheric levels and on their interaction with it.

The above-proposed ternary diagram ($Na_2O + K_2O$)–$Fe_2O_3^* \times 5$–($CaO + MgO$)$\times 5$, based on the molecular quantities

of rock-forming oxides, permits the reliable separation of *A*-type granitoids and felsic igneous rocks of other types. The recognized fields of *A*-type rocks correspond to two petrogenetic types: resulted from the differentiation of alkali-basaltic magmas with minor assimilation (A_1) and from the interaction of mantle melts with felsic continental crustal material accompanied by serious contamination (A_2). This diagram must be applied to interprete the geodynamic formation conditions with caution. It should be used as a tool for a comprehensive analysis of obtained geological, petrological, and geochemical information. Nevertheless, A_1-type rocks form mostly in the intraplate magmatism setting: in intraoceanic system (oceanic islands) or near the divergent boundaries of lithospheric plates in cold intracontinental rifts, whereas A_2-type rocks are generated in the postcollisional (or late-collision) setting as well as during the lithospheric-plate sliding and at the late stages of evolution of hot rift structures.

The petrochemical data must be interpreted with regard to the restrictions made by the author on the diagram testing: One should use only felsic igneous rocks containing >67 wt.% SiO_2; ignore rocks subjected to considerable secondary superposed alterations and volcanic glasses, fiammes, or their fragments as well as rocks with $SiO_2 > 80$ wt.% and liquation products; make statistical processing of data in the 95% confidence interval for each complex of igneous rocks in order to achieve the maximum reliability of analytical results; and carefully interpret the compositions of oxidized (magnetite) *A*-type granitoids (including postcollisional) because of the expanding (up to 10%) zone of their overlapping with highly differentiated *I*- and *S*-type granitoids in the lowermost part of the field of A_2-type granites.

References

Anderson, J.L., Bender, E.E., 1989. Nature and origin of Proterozoic *A*-type granitic magmatism in the southwestern United States of America. Lithos 23, 19–52.

Anfilogov, V.N., Bobylev, I.B., Bragina, G.I., 1982. Acid–base properties of silicate melts and role of volatiles in acid–base interaction, in: Fluids in Magmatic Processes [in Russian]. Nauka, Moscow, pp. 228–241.

Avanzinelli, R., Bindi, L., Menchetti, S., Conticelli, S., 2004. Crystallisation and genesis of peralkaline magmas from Pantelleria Volcano, Italy: an integrated petrological and crystal-chemical study. Lithos 73, 41–69.

Azer, M.K., 2007. Tectonic significance of Late Precambrian calc-alkaline and alkaline magmatism in Saint Katherina Area, Southern Sinai, Egypt. Geol. Acta 5, 255–272.

Bacon, C.R., MacDonald, R., Smith, R.L., Baedecker, P.A., 1981. Pleistocene high-silica rhyolites of the Coso Volcanic Field, Inyo County, California. J. Geophys. Res. 86, 10,223–10,241.

Baker, P.E., 1974. Peralkaline acid volcanic rocks of oceanic islands. Bull. Volcanol. 38, 737–754.

Barbarin, B., 1999. A review of the relationships between granitoid types, their origins and their geodynamic environments. Lithos 46, 605–626.

Barron, J., Larsen, B., Baldauf, J., Shipboard Scientific Party, 1991. Proceedings of the Ocean Drilling Program, Scientific Results. College Station, TX, Vol. 119, pp. 868–891.

Bea, F., 1996. Residence of REE, Y, Th, and U in granites and crustal protoliths, implications for the chemistry of crustal melts. J. Petrol. 37, 521–552.

Best, M.G., Christiansen, E.H., 1991. Limited extension during peak Tertiary volcanism, Great Basin of Nevada and Utah. J. Geophys. Res. 96, 13,509–13,528.

Bezmen, N.I., Zharikov, V.A., Zevel'sky, V.O., Kalinichev, A.G., 2005. Melting of alkali aluminosilicate systems under hydrogen–water fluid pressure, $P_{tot} = 2$ kbar. Petrology 13 (5), 407–426.

Bogatikov, O.A., Borsuk, A.M. (Eds.), 1987. Natural Glasses as Indicators of Geologic Processes [in Russian]. Nauka, Moscow.

Bonin, B., 2007. *A*-type granites and related rocks: evolution of a concept, problems and prospects. Lithos 97, 1–29.

Bonin, B., Grelou-Orsini, C., Vialette, Y., 1978. Age, origin and evolution of the anorogenic complex of Evisa (Corsica): a K-Li-Rb-Sr study. Contrib. Mineral. Petrol. 65, 425–432.

Botelho, N.F., Moura, M.A., 1998. Granite-ore deposit relationships in central Brazil. J. South Am. Earth Sci. 11, 427–438.

Bowden, P., Black, R., Martin, R.F., Ike, E.C., Kinnaird, J.A., Batchelor, R.A., 1987. Niger–Nigerian alkaline ring complexes: a classic example of African Phanerozoic anorogenic mid-plate magmatism, in: Fitton, J.G., Upton, B.G.J. (Eds.), Alkaline Igneous Rocks. Geol. Soc. London, Special Publ. 30, 357–379.

Breiter, K., 2012. Nearly contemporaneous evolution of the *A*- and *S*-type fractionated granites in the Krune hory/Erzgebirge Mts., Central Europe. Lithos 151, 105–121.

Buck, W.R., Martinez, F., Stecklear, M.S., Cochran, J.R., 1988. Thermal consequences of lithospheric extension: pure and simple. Tectonics 7 (2), 213–234.

Calzia, J.P., Ramo, O.T., 2005. Middle Miocene rapakivi granites of Death Valley, in: Calzia, J.P. (Ed.), Fifty Years of Death Valley Research: A Volume in Honor of Lauren A. Wright and Bennie Troxel. Earth-Sci. Rev. 73, 221–243.

Capaldi, G., Chiesa, S., Manetti, P., Orsi, G., Poli, G., 1987. Tertiary anorogenic granites of the western border of the Yemen Plateau. Lithos 20, 433–444.

Cathey, H.E., Nash, B.P., 2004. The Cougar Point Tuff: implications for thermochemical zonation and longevity of high-temperature, large-volume silicic magmas of the Miocene Yellowstone hotspot. J. Petrol. 45, 27–58.

Chappell, B.W., White, A.J.R., 1974. Two contrasting granite types. Pacific Geol. 8, 173–174.

Chappell, B.W., White, A.J.R., 1988. *I*- and *S*-type granites in the Lachlan Fold Belt. Trans. R. Soc. Edinb., Earth Sci. 79, 169–181.

Chappell, B.W., White, A.J.R., 1992. *I*- and *S*-type granites in the Lachlan Fold Belt. Trans. R. Soc. Edinb., Earth Sci. 83, 1–26.

Chetverikov, S.D., 1956. A Guide for Petrochemical Conversion of Analytical Data for Rocks and Determination of Their Chemical Types [in Russian]. Gosgeoltekhizdat, Moscow.

Christiansen, E.H., Haapala, I., Hart, G.L., 2007. Are Cenozoic topaz rhyolites the erupted equivalents of Proterozoic rapakivi granites? Examples from the western United States and Finland. Lithos 97, 219–246.

Coira, B., Kay, S.M., 1993. Implications of Quaternary volcanism at Cerro Tuzgle for crustal and mantle evolution of the Puna Plateau, Central Andes, Argentina. Contrib. Mineral. Petrol. 113, 40–58.

Collins, W.J., Beams, S.D., White, A.J.R., Chappell, B.W., 1982. Nature and origin of *A*-type granite with particular reference to southeastern Australia. Contrib. Mineral. Petrol. 80, 189–200.

Creaser, R.A., Price, R.C., Wormald, R.J., 1991. *A*-type granites revisited: assessment of a residual-source model. Geology 19, 163–166.

Dall'Agnol, R., Olivera, D.C., 2007. Oxidized, magnetite-series, rapakivi-type granites of Carajas, Brasil: implications for classification and petrogenesis of A-type granites. Lithos 93, 215–233.

Dobretsov, N.L., 2003. Mantle plumes and their role in the formation of anorogenic granitoids. Geologiya i Geofizika (Russian Geology and Geophysics) 44 (12), 1243–1261 (1199–1218).

Dobretsov, N.L., Koulakov, I.Yu., Litasov, Yu.D., 2012. Migration paths of magma and fluids and lava compositions in Kamchatka. Russian Geology and Geophysics (Geologiya i Geofizika) 53 (12), 1253–1275 (1633–1661).

Donskaya, T.G., Bibikova, E.V., Gladkochub, D.P., Mazukabzov, A.M., Bayanova, T.B., De Waile, B., Didenko, A.N., Bukharov, A.A., Kirnozova, T.I., 2008. Petrogenesis and age of the felsic volcanic rocks from the North Baikal volcanoplutonic belt, Siberian Craton. Petrology 16 (5), 422–447.

Donskaya, T.G., Gladkochub, D.P., Mazukabzov, A.M., Presnyakov, S.L., Bayanova, T.B., 2013. Paleoproterozoic granitoids of the Chuya and Kutima complexes (southern Siberian craton): age, petrogenesis, and geodynamic setting. Russian Geology and Geophysics (Geologiya i Geofizika) 54 (3), 283–296 (371–389).

Duchesne, J., Wilmart, E., 1997. Igneous charnockites and related rocks from the Bjerkreim–Sokndal layered intrusion (Southwest Norway): a jotunite (hypersthene monzodiorite)-derived A-type granitoid suite. J. Petrol. 38, 337–369.

Eby, G.N., 1992. Chemical subdivision of the A-type granitoids: petrogenetic and tectonic implications. Geology 20, 641–644.

Eby, G.N., Krueger, H.W., Creasy, J.W., 1992. Geology, geochronology, and geochemistry of the White Mountain batholith, New Hampshire, in: Puffer, J.H., Ragland, P.C. (Eds.), Eastern North American Mesozoic Magmatism. Geol. Soc. Am., Spec. Paper 268, 379–398.

Elliott, B.A., Peck, W.H., Ramo, O.T., Vaasjoki, M., Nironen, M., 2005. Magmatic zircon oxygen isotopes of 1.88–1.87 Ga orogenic and 1.65–1.54 Ga anorogenic magmatism in Finland. Mineral. Petrol. 85, 223–241.

Epel'baum, M., 1980. Volatile-Containing Silicate Melts [in Russian]. Nauka, Moscow.

Fletcher, C.J.N., Beddoe-Stephens, B., 1987. The petrology, chemistry and crystallization history of the Velasco alkaline province, eastern Bolivia, in: Fitton, J.G., Upton, B.G.J. (Eds.), Alkaline Igneous Rocks. Geol. Soc. London, Spec. Publ. 30, 403–414.

Fraga, L.M.B., Dall'Agnol, R., Costa, J.B.S., Macambira, M.J.B., 2009. The Mesoproterozoic Mucajai anorthosite–mangerite–rapakivi granite complex, Amazonian craton, Brazil. Can. Mineral. 47, 1469–1492.

Frindt, S., Haapala, I., Pakkanen, L., 2004. Anorogenic Gross Spitzkoppe granite stock in central western Namibia. Part I. Petrology and geochemistry. Am. Mineral. 89, 841–856.

Frost, B.R., Barnes, C.G., Collins, W.J., Arculus, R.J., Ellis, D.J., Frost, C.D., 2001. A geochemical classification for granitic rocks. J. Petrol. 42, 1771–1802.

Frost, C.D., Frost, B.R., 2011. On ferroan (A-type) granitoids: their compositional variability and modes of origin. J. Petrol. 52, 39–53.

Frost, C.D., Frost, B.R., Chamberlain, K.R., Edwards, B.R., 1999. Petrogenesis of the 1.43 Ga Sherman batholith, SE Wyoming: a reduced rapakivi-type anorogenic granite. J. Petrol. 40, 1771–1802.

Girard, G., Stix, J., 2010. Rapid extraction of discrete magma batches from a large differentiating magma chamber: the Central Plateau Member rhyolites, Yellowstone Caldera, Wyoming. Contrib. Mineral. Petrol. 160, 441–465.

Goodenough, K.M., Upton, B.G.J., Ellam, R.M., 2000. Geochemical evolution of the Ivigtut granite, South Greenland: a fluorine-rich "A-type" intrusion. Lithos 51, 205–221.

Grebennikov, A.V., 2003. Petrogenesis of Ignimbrites of the Yakut Volcanic Structure (Primorye). PhD Thesis. DVGI DVO RAN, Vladivostok.

Grebennikov, A.V., Maksimov, S.O., 2006. Fayalite rhyolites and a zoned magma chamber of the Paleocene Yakutinskaya volcanic depression in Primorye, Russia. J. Miner. Petrol. Sci. 101, 69–88.

Grebennikov, A.V., Popov, V.K., 2014. Petrogeochemical aspects of the Late Cretaceous and Paleogene ignimbrite volcanism of East Sikhote-Alin. Russian J. Pacific Geology 8 (1), 38–55.

Grebennikov, A.V., Shcheka, S.A., Karabtsov, A.A., 2012. Silicate–metallic spherules and the problem of mechanism of ignimbrite eruptions (by the

example of the Yakut volcanotectonic structure). Vulkanologiya i Seismologiya, No. 4, 1–20.

Haapala, I., Frindt, S., Kandara, J., 2007. Cretaceous Gross Spitzkoppe and Klein Spitzkoppe stocks in Namibia: topaz-bearing A-type granites related to continental rifting and mantle plume. Lithos 97, 174–192.

Harris, N.B.W., Pearse, J.A., Tindle, A.G., 1986. Geochemical characteristics of collision-zone magmatism, in: Cowards, M.P., Ries, A.C. (Eds.), Collisions Tectonics. Geol. Soc. London, Spec. Publ. 19, 67–81.

Heilimo, E., Halla, J., Lauri, L.S., Ramo, O.T., Huhma, H., Kurhila, M.I., Front, K., 2009. The Paleoproterozoic Nattanen-type granites in northern Finland and vicinity—a postcollisional oxidized A-type suite. Bull. Geol. Soc. Finland 81, 7–38.

Ishihara, S., 1977. The magnetite-series and ilmenite-series granitic rocks. Mining Geol. 27, 293–305.

Ivanov, K.S., Erokhin, Yu.V., Ronkin, Yu.L., Khiller, V.V., Rodionov, N.V., Lepikhina, O.P., 2012. The first data on the Early Proterozoic sialic basement in the eastern West Siberian Platform (studies of the Tyn'yar rhyolite–granite pluton). Russian Geology and Geophysics (Geologiya i Geofizika) 53 (10), 997–1011 (1304–1321).

Janasi, V., Vlach, S.R.F., Campos Neto, M., Ulbrich, H.G.J., 2009. Associated A-type subalkaline and high-K calc-alkaline granites in the Itu granite province, southeastern Brazil: petrological and tectonic significance. Can. Mineral. 47, 1505–1526.

Jones, C.H., Unruh, J.R., Sonder, L.J., 1996. The role of gravitational potential energy in active deformation in the southwestern United States. Nature 381, 37–41.

Karsten, M., Baker, P.E., Buckley, Fl., 1974. Petrology and geochemistry of Easter Island. Contrib. Mineral. Petrol. 44, 85–100.

Kaur, P., Chaudhri, N., Okrusch, M., Koepke, J., 2006. Palaeoproterozoic A-type felsic magmatism in the Khetri Copper Belt, Rajasthan, northwestern India: petrologic and tectonic implications. Mineral. Petrol. 87, 81–122.

Khanchuk, A.I., Golozubov, V.V., Martynov, Yu.A., Simanenko, V.P., 1997. Early Cretaceous and Paleogene transform continental margins (Californian type) of the Russian Far East, in: Tectonics of Asia [in Russian]. GEOS, Moscow, pp. 240–243.

Kieffer, B., Arnd, N.T., Weis, D., 2002. A bimodal alkalic shield volcano on Skiff Bank: its place in the evolution of the Kerguelen Plateau. J. Petrol. 43, 1259–1286.

Kisvarsanyi, E.B., Kisvarsanyi, G., 1990. Alkaline granite ring complexes and metallogeny in the Middle Proterozoic St. Francois terrane, southeastern Missouri, U.S.A, in: Gower, C.F., Rivers, T., Ryan, B. (Eds.), Mid-Proterozoic Laurentia–Baltica. Geol. Assoc. Canada, Spec. Paper 38, 433–446.

Konopelko, D., Biske, G., Seltmann, R., Eklund, O., Belyatsky, B., 2007. Hercynian postcollisional A-type granites of the Kokshaal Range, Southern Tien Shan, Kyrgyzstan. Lithos 97, 140–160.

Kumar, K.V., Frost, C.D., Frost, B.R., Chamberlain, K.R., 2007. The Chimakurti–Errakonda–Uppalapadu plutons, Eastern Ghats Belt, India: an unusual association of tholeiitic and alkaline magmatism. Lithos 97, 30–57.

Kuz'min, M.I., 1985. Geochemistry of Igneous Rocks of Phanerozoic Mobile Belts [in Russian]. Nauka, Novosibirsk.

Lauri, L.S., Ramo, O.T., Huhma, H., Manttari, I., Rasanen, J., 2006. Petrogenesis of silicic magmatism related to the 2.44 Ga rifting of Archean crust in Koillismaa, eastern Finland. Lithos 86, 137–166.

Leonov, V.L., Grib, E.N., 2004. Structural Positions and Volcanism of Quaternary Calderas in Kamchatka [in Russian]. Dal'nauka, Vladivostok.

Litvinovsky, B.A., Jahn, B., Zanvilevich, A.N., Saunders, A., Poulain, S., Kuzmin, D.V., Reichow, M.K., Titov, A.V., 2002. Petrogenesis of syenite–granite suites from the Bryansky Complex (Transbaikalia, Russia): implications for the origin of A-type granitoid magmas. Chem. Geol. 189, 105–133.

Loiselle, M.C., Wones, D.R., 1979. Characteristics and origin of anorogenic granites, in: Abstracts of Papers to Be Presented at the Annual Meetings of the Geological Society of America and Associated Societies. San Diego, California, Vol. 11, November 5–8, p. 468.

MacDonald, R.M., Davies, G.R., Bliss, C.M., Leat, P.T., Bailey, D.K., Smith, R.L., 1987. Geochemistry of high-silica peralkaline rhyolites, Naivasha, Kenya Rift Valley. J. Petrol. 28, 979–1008.

Maeda, J., 1990. Opening of the Kuril Basin deduced from the magmatic history of central Hokkaido, North Japan. Tectonophysics 174, 235–255.

Maniar, P.D., Piccolli, P.M., 1989. Tectonic discrimination of granitoids. Geol. Soc. Am. Bull. 101, 635–643.

Mikhailov, V.A., 1989. Magmatism of Volcanotectonic Structures in the South of the East Sikhote-Alin Volcanic Belt [in Russian]. DVO AN SSSR, Vladivostok.

Naumov, V.B., Kovalenko, V.I., Dorofeeva, V.A., Girnis, A.V., Yarmolyuk, V.V., 2010. Average compositions of igneous melts from main geodynamic settings according to the investigation of melt inclusions in minerals and quenched glasses of rocks. Geochem. Int. 48 (12), 1185–1207.

Nozhkin, A.D., Turkina, O.M., Bayanova, T.B., Berezhnaya, N.G., Larionov, A.N., Postnikov, A.A., Travin, A.V., Ernst, R.E., 2008. Neoproterozoic rift and within-plate magmatism in the Yenisei Ridge: implications for the breakup of Rodinia. Russian Geology and Geophysics (Geologiya i Geofizika) 49 (7), 503–519 (666–688).

Ogunleyea, P.O., Ikeb, E.C., Garba, I., 2005. Geochemical characteristics of the niobium-rich arfvedsonite granites, Younger Granites province of Nigeria. Chemie der Erde 65, 279–296.

O'Halloran, D.A., 1985. Ras ed Dom migrating ring complex: *A*-type granites and syenites from the Bayuda Desert, Sudan. J. Afric. Earth Sci. 3, 61–75.

Orajaka, I.P., 1986. Geochemistry of Kaffo Valley albite–riebeckite–granite, Liruei granite ring-complex, northern Nigeria. Chem. Geol. 56, 85–92.

Patoka, M.G., 1983. Pliocene–Quaternary Felsic Alkaline Rocks of the Central Part of the Sredinnyi Ridge, Kamchatka. PhD Thesis [in Russian]. DVNTs AN SSSR, Petropavlovsk-Kamchatskii.

Pearce, J.A., Harris, N.B.W., Tindle, A.G., 1984. Trace element discrimination diagrams for the tectonic interpretation of granitic rocks. J. Petrol. 25, 956–983.

Pichler, H., Zeil, W., 1971. The Cenozoic rhyolite–andesite association of the Chilean Andes. Bull. Volcanol. 35, 424–452.

Pokrovskii, B.G., 2000. Crustal Contamination of Mantle Magmas: Data of Isotope Geochemistry [in Russian]. Nauka/Interperiodika, Moscow.

Pollard, P.J., 2006. An intrusion-related origin for Cu–Au mineralization in iron oxide–copper–gold (IOCG) provinces. Mineral. Deposita 41, 179–187.

Popov, V.K., Sakhno, V.G., Kuzmin, Ya.V., Glascock, M.D., Choi, B.K., 2005. Geochemistry of volcanic glasses from the Paektusan Volcano. Dokl. Earth Sci. 403 (5), 803–807.

Pritchard, C.J., Larson, P.B., 2012. Genesis of the post-caldera eastern Upper Basin Member rhyolites, Yellowstone, WY: from volcanic stratigraphy, geochemistry, and radiogenic isotope modeling. Contrib. Mineral. Petrol. 164, 205–228.

Radain, A.A.M., Fyfe, W.S., Kerrich, R., 1981. Origin of peralkaline granites of Saudi Arabia. Contrib. Mineral. Petrol. 78, 358–366.

Rogers, J.J.W., Greenberg, J.E., 1990. Late-orogenic, post-orogenic, and anorogenic granites: distinction by major-element and trace-element chemistry and possible origins. J. Geol. 98, 291–310.

Rudnev, S.N., Babin, G.A., Vladimirov, A.G., Kruk, N.N., Shokal'sky, S.P., Borisov, S.M., Travin, A.V., Levchenkov, V.A., Terleev, A.A., Kuibida, M.L., 2005. Geologic setting, age, and geochemical model of the formation of West Sayan plagiogranitoids. Geologiya i Geofizika (Russian Geology and Geophysics) 46 (2), 170–187 (169–187).

Savel'eva, V.B., Bazarova, E.P., 2012. The Early Proterozoic Primorskii complex of rapakivi granites (western Cisbaikalia): geochemistry, crystallization conditions, and ore potential. Russian Geology and Geophysics (Geologiya i Geofizika) 53 (2), 147–168 (193–218).

Sklyarov, E.V., Mazukabzov, A.M., Mel'nikov, A.I., 1997. Complexes of Metamorphic Cores of the Cordilleran Type [in Russian]. Izd. SO RAN, NITs OIGGM SO RAN.

Smith, D.R., Noblett, J., Wobus, R.A., Unruh, D., Douglass, J., Beane, R., Davis, C., Goldman, S., Kay, G., Gustavson, B., Saltoun, B., Stewart, J., 1999. Petrology and geochemistry of late-stage intrusions of the *A*-type, mid-Proterozoic Pikes Peak batholith (Central Colorado, USA): implications for petrogenesis models. Precam. Res. 98, 271–305.

Smith, I.E.M., Chappell, B.W., Ward, G.K., Freeman, R.C., 1977. Peralkaline rhyolites associated with andesitic arcs of the Southwest Pacific. Earth Planet. Sci. Lett. 37, 230–236.

Smith, R.B., Jordan, M., Steinberger, B., Puskas, C.M., Farrell, J., Waite, G.P., Husen, S., Chang, W-L., O'Connell, R., 2009. Geodynamics of the Yellowstone hotspot and mantle plume: seismic and GPS imaging, kinematics, and mantle flow. J. Volcanol. Geotherm. Res. 188, 26–56.

Suwa, K., Tokieda, K., Hoshino, M., 1994. Palaeomagnetic and petrological reconstruction of the Seychelles. Precam. Res. 69, 281–292.

Sylvester, P.J., 1989. Post-collisional alkaline granites. J. Geol. 97, 261–280.

Tommasini, S., Poli, G., Manetti, P., Conticelli, S., 1994. Oligo-Miocene *A*-type granites and granophyres from Yemen: isotopic and trace-element constraints bearing on their genesis. Eur. J. Miner. 6, 571–590.

Trua, T., Deniel, C., Mazzuoliet, R., 1999. Crustal control in the genesis of Plio-Quaternary bimodal magmatism of the Main Ethiopian Rift (MER): geochemical and isotopic (Sr, Nd, Pb) evidence. Chem. Geol. 155, 201–231.

Trunilina, V.A., Orlov, Yu.S., Roev, S.P., Zaitsev, A.I., 2008. Composition and genetic aspects of formation of *A*-type granitoids in the Upper Yana–Kolyma folded area. Otechestvennaya Geologiya, No. 5, 99–109.

Turkina, O.M., Nozhkin, A.D., Bayanova, T.B., 2006. Sources and formation conditions of Early Proterozoic granitoids from the southwestern margin of the Siberian craton. Petrology 14 (3), 262–283.

Velikoslavinskii, S.D., 2003. Geochemical classification of silicic igneous rocks of major geodynamic environments. Petrology 11 (4), 327–342.

Verma, S.P., Pandarinath, K., Verma, S.K., Agrawal, S., 2013. Fifteen new discriminant-function-based multi-dimensional robust diagrams for acid rocks and their application to Precambrian rocks. Lithos 168–169, 113–123.

Vernikovskaya, A.E., Vernikovsky, V.A., Sal'nikova, E.B., Kotov, A.B., Kovach, V.P., Travin, A.V., Wingate, M.T.D., 2007. *A*-type leucogranite magmatism in the evolution of continental crust on the western margin of the Siberian craton. Russian Geology and Geophysics (Geologiya i Geofizika) 48 (1), 3–16 (5–21).

Vetrin, V.R., Berezhnaya, N.G., Rodionov, N.V., 2006. Petrology of postorogenic granitoids of the Northern Baltic Shield. Dokl. Earth Sci. 411 (6), 1476–1479.

Whalen, J.B., Currie, K.L., Chappell, B.W., 1987. *A*-type granites: geochemical characteristics, discrimination and petrogenesis. Contrib. Mineral. Petrol. 95, 407–419.

Woolley, A.R., Jones, G.C., 1987. The petrochemistry of the northern part of the Chilwa alkaline province, Malawi, in: Fitton, J.G., Upton, B.G.J. (Eds.), Alkaline Igneous Rocks. Geol. Soc. London, Spec. Publ. 30, 335–356.

Wormald, R.J., Price, R.C., 1988. Peralkaline granites near Temora, southern New South Wales: tectonic and petrological implications. Aust. J. Earth Sci. 35, 209–221.

Yang, J.-H., Wu, F.-Y., Chung, S.-L., Wilde, S.A., Chu, M.-F., 2006. A hybrid origin for the Qianshan *A*-type granite, northeast China: geochemical and Sr–Nd–Hf isotopic evidence. Lithos 89, 89–106.

Yarmolyuk, V.V., Kovalenko, V.I. (Eds.), 1987. Igneous Rocks. Felsic and Intermediate Rocks [in Russian]. Nauka, Moscow, Vol. 4.

Yarmolyuk, V.V., Kovalenko, V.I. (Eds.), 1991. Rift Magmatism of Active Continental Margins and Its Ore Potential [in Russian]. Nauka, Moscow.

Editorial responsibility: E.V. Sklyarov